




Lipid Microparticles Show Similar Efficacy With Lipid Nanoparticles in Delivering mRNA and Preventing Cancer

Afang Ji^{1,2} · Minghao Xu^{1,2,3} · Yunzhi Pan^{2,4} · Lu Diao^{3,4} · Lin Ma⁴ · Li Qian⁴ · Junping Cheng^{1,2} · Mi Liu^{3,4} 

Received: 3 June 2022 / Accepted: 20 November 2022 / Published online: 30 November 2022
© The Author(s), under exclusive licence to Springer Science+Business Media, LLC, part of Springer Nature 2022

Abstract

Purpose Messenger RNA (mRNA) has shown great promise for vaccine against both infectious diseases and cancer. However, mRNA is unstable and requires a delivery vehicle for efficient cellular uptake and degradation protection. So far, lipid nanoparticles (LNPs) represent the most advanced delivery platform for mRNA delivery. However, no published studies have compared lipid microparticles (LMPs) with lipid nanoparticles (LNPs) in delivering mRNA systematically, therefore, we compared the impact of particle size on delivery efficacy of mRNA vaccine and subsequent immune responses.

Methods Herein, we prepared 3 different size lipid particles, from nano-sized to micro-sized, and they loaded similar amounts of mRNA. These lipid particles were investigated both *in vitro* and *in vivo*, followed by evaluating the impact of particle size on inducing cellular and humoral immune responses.

Results In this study, all mRNA vaccines showed a robust immune response and lipid microparticles (LMPs) show similar efficacy with lipid nanoparticles (LNPs) in delivering mRNA and preventing cancer. In addition, immune adjuvants, either toll like receptors or active molecules from traditional Chinese medicine, can improve the efficacy of mRNA vaccines.

Conclusions Considering the efficiency of delivery and endocytosis, besides lipid nanoparticles with size smaller than 150 nm, lipid microparticles (LMPs) also have the potential to be an alternative and promising delivery system for mRNA vaccines.

Keywords lipid microparticles · lipid nanoparticles · LMP · LNP · mRNA vaccine · particle size

Introduction

Vaccines are widely considered one of the greatest public health achievements and vaccinations have greatly decreased the burden of infectious diseases worldwide and

saved millions of lives each year [1–3]. A novel coronavirus, severe acute respiratory syndrome coronavirus 2 (SARS-CoV-2) has caused a pandemic world-wide and caused millions of deaths. Given that vaccines are the most important public health approach to protect people from COVID-19, companies and research institutions competitively devoted to develop SARS-CoV-2 vaccines. So far, researchers have developed inactivated vaccines, viral-vector-based vaccine, subunit vaccines and mRNA vaccines etc. [3–5]. Among them, mRNA vaccines showed excellent efficacy and showed potentials in application beyond preventing infection disease. In addition to infectious diseases, mRNA vaccines can also be used to treat other diseases, such as cancer [4–6].

According to recent studies, nucleic acid-based vaccines could provide efficient protection or treatment, by stimulating both humoral immunity and cellular immunity [7]. Compared to DNA vaccines, mRNA vaccines demonstrated significant advantages, in terms of its high potency, capacity for rapid development and potential for low-cost manufacture and safe administration [4, 7, 8]. The technical challenges associated

Afang Ji, Minghao Xu, Yunzhi Pan contributed equally to the work.

✉ Junping Cheng
19828955@qq.com

✉ Mi Liu
mi.liu@suda.edu.cn

¹ Suzhou TCM Hospital Affiliated to Nanjing University of Chinese Medicine, Suzhou 215000, Jiangsu, China

² The Fifth People's Hospital of Suzhou, Suzhou 215000, Jiangsu, China

³ Suzhou Ersheng Biopharmaceutical Co., Ltd, Suzhou 215000, People's Republic of China

⁴ College of Pharmaceutical Science, Soochow University, Suzhou 215123, Jiangsu, China

with DNA vaccines are to ensure delivery into the cell nucleus potential risks of integration into the host genome. While mRNA has no potential risks of infection or genomic integration, thanks to mRNA carries genetic information from the DNA to the cytosol, where it is used by the ribosomes as a template for protein synthesis [3, 6, 9, 10]. Furthermore, mRNA can be degraded by normal cellular processes, and the half-life of mRNA can be regulated through the use of various modifications and delivery methods [3, 11, 12].

However, therapeutics based on mRNA has the challenges of the instability of mRNA and the crossing of membrane barrier [3, 9, 12]. Recent technological advances have now largely overcome these issues, these new technologies include mRNA modification and delivery platforms such as protamine complexes, nanoparticles based on lipids or polymers, and hybrid formulations etc [11–16]. Indeed, a good delivery platform should efficiently bind mRNA, protect mRNA from extracellular RNase degradation, uptake by the desired target cell and express the mRNA in target cells [17]. So far, lipid nanoparticles (LNPs) is the most promising and developed technology for mRNA delivery [16, 18, 19]. A typical lipid/mRNA particles formulation is consisted of ionizable lipids or cationic lipids, neutral helper lipids, sterol lipid and a polyethylene glycol (PEG)-lipid [20–23]. It is reported that mRNA vaccines delivered by lipid/mRNA particles can activate both humoral and cellular immune responses potently. Many factors may affect the potency of mRNA vaccine delivered by lipid/mRNA particles, such as particle size and the incorporation of adjuvants [23, 24].

In previous studies and the FDA-approved mRNA vaccines, researcher applied lipid nanoparticles with the size around 70 nm–100 nm. Though the scientists from Moderna analyzed lipid nanoparticles range from 50 to 200 nm and proved that LNPs, with size from 50 to 200 nm, yielded similar robust immune response [20, 25]. However, no studies have compared the impact of particle size, in a broader range, on the efficacy of lipid particles. Given that the size of particles can impact the migration and uptake of particles, particles with size larger than 200 nm may have particular behaviors [1, 26]. So far, the studies of vaccine delivery by microparticles focus on biodegradable materials-based microparticles, such as PLGA microparticles and the payload of microparticles focus on protein or peptide antigens. Recently, a few siRNA delivery by microparticles have been explored and these limited number studies of siRNA delivery by microparticles focus on pulmonary administration or lung-targeting [27–30]. No studies have evaluated the delivery efficacy of mRNA vaccines by microparticles, especially lipid microparticles. Studies have reported that microparticles, loaded with antigens, might have the advantages in activating immune responses, such as microparticles degrade more slowly and can be more taken up by antigen presenting cells, besides endocytosis microparticles can also attach to the surface of

antigen presenting cells and deliver antigens, microparticles produced enhanced CD4+ T cell activation compared to smaller size nanoparticles etc [1, 26, 30–41]. Therefore, delivery of mRNA vaccines by microparticles might be a promising strategy for mRNA drugs. Herein, we evaluated the impact of particle size, especially larger size, on cellular uptake and immune responses induction of mRNA lipid particles in a broader size range. Especially, we compared the efficacy of lipid microparticles (LMPs) with LNPs in delivering mRNA.

To our knowledge, the most commonly used lipid particles for mRNA delivering are about 50 nm–100 nm, hence 70 nm–100 nm was chosen as the small size of lipid nanoparticles (LNPs). Considering other common applied nanoparticle size, we selected 250 nm–350 nm as the size for medium size lipid nanoparticles (LNPs) and selected 1.1 μm –1.3 μm as the size for large size lipid microparticles (LMPs).

In order to specifically investigate the impact of particle size on vaccine potency, all other factors of the delivery system must be matched [25, 42]. In our study, we changed lipid/mRNA nanoparticles/microparticles size independent of lipid composition by different preparation methods. The different size lipid/mRNA particles with or without adjuvants were prepared by using solvent diffusion method, microfluidics and film dispersion method. To investigate the impact of particle size and adjuvants on the efficacy of mRNA vaccine, we immunized mice with mRNA vaccine encodes ovalbumin (OVA) and then challenge mice with subcutaneously inoculation of OVA expressing E.G7 lymphoma cells. Both lipid nanoparticles and lipid microparticles were investigated and both poly(I:C) and hesperetin were tested when work as adjuvants. According to the results, both poly(I:C) and hesperetin can be used as immune adjuvants to enhance the potency of lipid/mRNA complexes, and all size lipid/mRNA nanoparticles/microparticles produced robust immune responses.

Materials & Methods

Materials

DOTAP, DOPE and DMG-PEG2000 were purchased from Avanti Polar Lipids (Alabama, USA); cholesterol was purchased from Sinopharm Chemical Reagent (China); FITC-DSPE-PEG2000 was obtained from AVT (Shanghai, China); Hesperetin was produced in Yuanye (Shanghai, China); eGFP mRNA was obtained from VectorBuilder (Guangzhou, China); OVA mRNA was purchased from TriLink Bio Technologies (California, USA); Quanti-iT RiboGreen RNA reagent and Kit were obtained from Invitrogen (California, USA); Mouse ovalbumin specific IgG ELISA kit was purchased from Shanghai Enzyme-linked Biotechnology (Shanghai, China);

OVA323-339, OVA257-264, OVA208-216, OVA27-35 were purchased from Apeptide (Shanghai, China); Poly(I:C) (HMW) VacciGrade™ was obtained from InvivoGen (San Diego, USA); DMEM medium, RPMI 1640 medium, 1% Penicillin/Streptomycin, PBS and FBS were purchased from Procell Life Science&Technology (Wuhan, China).

Cell Culture and Animal Studies

DC2.4 (American Type Culture Collection, Manassas, VA, USA) was cultured in the Dulbecco's Modified Eagle Medium (DMEM) containing 10% Fetal Bovine Serum (FBS) and 1% Penicillin/Streptomycin (P/S) (Procell Life Science&Technology Co., Ltd., China) in 5% CO₂ at 37°C. RPMI 1640 medium containing 10% FBS and 1% PS was used to culture E.G7-OVA cells (BeNa Culture Collection, China). For *in vivo* assays, 6–8 weeks old female C57BL/6 mice were used. Mice were assigned to treatment groups based on cage numbers. All animal work was approved and monitored by the Animal Ethics Committee of Soochow University. All the mice were ordered from the animal facility platform of Soochow University.

Lipid/mRNA Nanoparticle/Microparticle Preparation

Lipid/mRNA complexes with different particle size were formulated by solvent diffusion method, microfluidics or film dispersion method. The ethanol phase was prepared by solubilizing a mixture of cationic lipid (DOTAP, Avanti Polar Lipids, USA), DOPE (Avanti Polar Lipids), cholesterol (Sinopharm Chemical Reagent Co., Ltd, China) and DMG-PEG2000 (Avanti Polar Lipids) at a molar ratio of 35:16:46.5:2.5 with ethanol; hesperetin (5 mg/mL) was also solved in the ethanol phase in the particles loaded with hesperetin as immune adjuvants. The aqueous phase was prepared in 10 mM citrate buffer (pH 3) with either EGFP mRNA (VectorBuilder, USA) or OVA mRNA (TriLink Bio-Technologies, USA), with or without poly(I:C) (1 mg/mL).

Small size lipid/mRNA nanoparticles were prepared via solvent diffusion method by mixing the aqueous phase and ethanol phase in volumetric flow ratios 4:1 and heating the mixture to 55°C for 10 min. Medium size lipid/mRNA nanoparticles were prepared via microfluidics by mixing the aqueous phase and ethanol phase in volumetric flow ratios 3:1. Large lipid/mRNA microparticles were prepared via film dispersion method. Heating the ethanol phase to 40°C for 30 min to form a lipid film and adding the aqueous phase to dissolve the film. The molar ratio between mRNA and the cationic lipid was 1:20. The prepared lipid complexes were purified by dialyzing against 1 × PBS solution in a 1000 MWCO dialysis membrane (Spectrum Laboratories, Inc, USA) at 4°C for 2 h. Before the administration of mRNA lipid particles loaded with

poly(I:C) as immune adjuvants, Lipid/ mRNA particles were mixed with 0.1 mL poly(I:C) to load poly(I:C) to the exterior part of the lipid particle.

The lipid particles loaded with dyes were prepared the same as described above, but replacing corresponding lipids with FITC-conjugated lipids.

Lipid/mRNA Nanoparticle/Microparticle Characterization

The size and surface charge of lipid particle were assessed with or without mRNA. The size, polydispersity (PDI) and Zeta potential of the lipid/mRNA particle were measured by a Zeta sizer Nano ZS (Malvern Instruments, UK).

A Quanti-iT RiboGreen RNA reagent and Kit (Invitrogen Corporation, USA) was used to calculate the mRNA encapsulation efficiency. The samples were diluted to a concentration of approximately 5 µg/mL in 1 × TE buffer solution. 50 µL of the diluted samples were transferred into a 96 well plate and either 50 µL of 1 × TE buffer solution (measuring “free” mRNA) or 50 µL of a 2% Triton-X100 (measuring total mRNA) was added to the certain wells. The plate was incubated at a temperature of 37°C for 15 min. The RiboGreen RNA reagent was diluted 1:100 in 1 × TE buffer solution, and 100 µL of this solution was added to each well. The fluorescence intensity was measured using the SPARK® multimode microplate reader (Tecan Trading AG, Switzerland) at an excitation wavelength of about 480 nm and an emission wavelength of about 520 nm. The fluorescence values of the reagent blank were subtracted from that of each of the samples. The percentage of free mRNA was determined by dividing the fluorescence intensity of the sample without Triton-X100 by the fluorescence intensity of the sample with Triton-X100.

The morphology of Lipid/mRNA complexes with different particle size were investigated by the transmission electron microscope (TEM). The samples were diluted to a concentration of approximately 100 µg/mL in deionized water (total lipid concentration was approximately 3.8 mg/mL). After dropping 10–20 µL diluted samples onto the copper nets, the nets were dried at 50–60°C for 3 h. Phosphotungstic acid solution (1%) was added to the prepared copper nets, 1–2 min later, using the filter paper to absorb the excess dyeing solution. The nets were washed 3 times and dried, followed by taking the images.

The stability analysis of LNPs and LMPs on particle size were conducted under 4°C and -20°C. The LNPs and LMPs were formulated as originally described and then stored in the refrigerator (4°C), or in the freezer (-20°C) for 4 weeks. Size was measured using a Malvern Zetasizer Nano (Malvern Instruments, UK) every week. Each LNP sample was measured three times.

***In Vitro* Cellular Uptake FITC-Lipid Nanoparticles/Microparticles**

Either DC2.4 cells and splenocytes from the mice were applied to conduct the uptake study. Splenocytes were isolated from sacrificed mice by using a 70 µm cell strainer (Sorfa Life Science Research Co., Ltd., China). After the isolation, red blood cells were lysed by using lysing buffer (BD Bioscience). After that, splenocytes were seeded into a 24-well plate at a density of 2.0×10^5 [5] cells/well and cell culture was done in 1.5 mL culture medium for 24 h at 37°C.

The blank lipid particles covalently modified with FITC were added into the DC2.4 cells or splenocytes, and then the cells were treated with 2 µg of the FITC- lipid particles for 4 h at 37°C in a CO₂ incubator.

After the incubation, DC2.4 cells were washed with PBS, collected and measured by using BD FACSAria™ III Cell Sorter Flow Cytometer (BD, USA).

In terms of splenocytes, the cells were washed with PBS, followed by staining with Zombie Aqua™ Fixable Viability Kit (BioLegend, USA) and incubating with Fc block for 10 min. Then, the splenocytes were stained with PerCP/Cyanine5.5 anti-mouse CD11c antibody, APC anti-mouse B220 antibody and PE anti-mouse F4/80 antibody in FACS buffer (1% FBS in PBS). After cell staining, the stained cells were washed with FACS buffer and measured by using Flow Cytometer.

Study of Transfection Efficacy *In Vitro*

DC2.4 cells were seeded into a 24-well plate at a density of 5×10^4 cells/well and cell culture was done in 1.5 mL Dulbecco's Modified Eagle Medium (DMEM) medium for 24 h at 37°C in a CO₂ incubator. Prior to transfections, EGFP mRNA encapsulated in lipid particles were added into cells in DMEM medium and incubated for 24 h at 37°C. After incubation, each well was imaged under a microscopy and flow cytometry was performed to measure the percentage of GFP-positive cells.

The transfection efficacy of lipid particles in DC, B cells and macrophage were compared by incubating splenocytes with different lipid particles. Splenocytes were prepared by isolating them from sacrificed mice and filtering through a 70 µm cell strainer (Sorfa Life Science Research Co., Ltd., China), followed by lysing red blood cells by using lysing buffer (BD Bioscience). After that, splenocytes were seeded into a 6-well plate at a density of 1.0×10^6 cells/well at 37°C. EGFP-mRNA encapsulated lipid particles were added into cells in DMEM medium (0.5 µg/mL) and incubated for 36 h at 37°C. After the incubation, splenocytes were washed with PBS, followed by staining with Zombie Aqua™ Fixable Viability Kit (BioLegend, USA) and incubating with Fc block for 10 min.

Then, the splenocytes were stained with CD11c-PE/Cy7, F4/80-PE and B220-PerCP/cy5.5 antibody (anti-mouse) in FACS buffer (1% FBS in PBS). After cell staining, the stained cells were washed with FACS buffer and measured by using BD FACSAria™ III Cell Sorter Flow Cytometer (BD, USA).

Analysis of Lipid Nanoparticles/Microparticles Uptake by Antigen-Presenting Cells *In Vivo*

Female C57BL/6 mice (6–8 weeks) were housed in groups of 5 mice per individually ventilated cage in an SPF facility. Mice were subcutaneous injected with FITC- lipid nanoparticles/microparticles. After 16 h, spleen and axillary lymph nodes were collected and processed into single-cell suspensions as previously described. Single-cell suspensions were stained with Zombie Aqua™ Fixable Viability Kit according to the manufacturer's instructions to exclude dead cells from analysis. After incubated with Fc-block to block nonspecific FcR binding, cells were surface stained with PerCP/Cyanine5.5 anti-mouse CD11c antibody, APC anti-mouse B220 antibody, APC/Cyanine7 anti-mouse F4/80 antibody and PE anti-mouse CD8a antibody for 30 min at 4°C. After cell staining, the stained cells were washed with FACS buffer and analyzed by flow cytometer.

Analysis of Biodistribution of Lipid Particles

The DiR dye (purchased from absin, abs45153692) was dissolved in ethanol to prepare a concentration of 1 mg/ml and the DiR dye was encapsulated into 3 different lipid particles with the above method. Female BALB/c mice aged 6–8 weeks received DiR via subcutaneously injected with lipid particles loaded with DiR dye, respectively. Imaging *in vivo* was performed at 6 h, 24 h and 48 h after injection. Meanwhile, the heart, liver, spleen, lung, kidney, draining lymph nodes and non-draining lymph nodes were taken out after 48 h to observe the distribution of DiR loaded in 3 different lipid particles. Fluorescence signals (Ex740nm, Em790nm) were measured by IVIS® Spectrum (PerkinElmer, Waltham, USA).

Immunization of Mice With Lipid Nanoparticles/Microparticles

Lipid nanoparticles/microparticles loading with OVA-mRNA and poly(I:C) (HMW) VacciGrade™ (InvivoGen, USA) or hesperetin (Yuanye, China) were used to immunize the mice. The C57BL/6 mice were randomized in different treatment groups and subcutaneously injected with mRNA vaccines near the inguinal lymph nodes twice at a weekly interval. Each dose contained 10 µg of mRNA, in the

administration with immune adjuvants each dose contained hesperetin 80 µg or 62.5 µg poly(I:C). The body weight of mice were recorded every week.

Challenge Immunized Mice With Inoculation of Tumor Cells

Mice were injected subcutaneously, on the flank of mice, with 3.0×10^5 E.G7-OVA cells 4 weeks after the first injection of mRNA vaccines. Tumor volume and body weight of the mice were measured every 3 days. The tumor size measurement was stopped when tumor size was exceeded 2000 mm³.

Analysis of Cellular Immunity Induced by mRNA Vaccines on Mice

The antigen-specific T cells in splenocytes were detected to analyze the cellular immunity induced by mRNA vaccines. Mice were sacrificed when the tumor size exceeded 2000 mm³ and splenocytes were collected, followed by processing into single-cell suspensions by using a 70 µm cell strainer and lysing buffer. And then, cells were seeded into a 12-well plate at a density of 2.0×10^5 cells/well and cell resting was done in 2 mL medium for 12 h at 37°C. After that, the isolated splenocytes were stimulated with peptide antigens (OVA323-339, OVA257-264, OVA208-216, OVA27-35, 10 µg/mL each, Apeptide, China) for 1 h at 37°C in a CO₂ incubator. After adding Brefeldin A (Bio-Legend, USA) for additional 11 h, the cells were washed with PBS and collected. Single-cell suspensions were then stained with Zombie Aqua™ Fixable Viability Kit and incubated with Fc block to block, followed by staining with APC anti-mouse CD3 antibody, Pacific Blue anti-mouse CD4 antibody, PE anti-mouse CD8a antibody and PE/Cy7 anti-mouse IFN-γ antibody prior to flow cytometry analysis.

Analysis of Humoral Immune Responses Induced by mRNA Vaccines on Mice

The antigen-specific antibody induced by mRNA vaccines was evaluated by Enzyme linked immunosorbent assay (ELISA). Approximately 200 µL of blood was collected 3 weeks after the second injection of mRNA vaccines for the measurement. After 2 h of incubation at 37°C, the collected blood was centrifuged at 1200 g for serum isolation (10 min at 4°C). Mouse ovalbumin specific IgG concentrations in serum were measured by ELISA kit (Shanghai Enzyme-linked Biotechnology Co., Ltd., China). Briefly, 96-well plates were coated with Ovalbumin. Serial dilutions of serum were added and enzyme-conjugate were added. Then covered with an

adhesive strip and incubated for 60 min at 37°C. After the incubation, the plate was washed 5 times with wash buffer. Substrate solution was then added to each well and incubated for 15 min. The reaction was stopped with adding stop solution. Finally, the plate was read at 450 nm absorbance using microplate reader. In each group, samples were analyzed in triplicate. Then construct the standard curve and calculate concentrations according to the manufacturer's instructions.

Analysis of Toxicity of Vaccines by Histological Analysis

Tumor-bearing mice were sacrificed when the tumor size exceeded 2000 mm³. Heart, liver, spleen, lung and kidney tissues were collected from tumor-bearing mice and healthy mice. These organs were embedded in paraffin and then the tissue sections were stained and analysis with H&E method.

Statistical Analysis

All data were evaluated and plotted by using GraphPad Prism 8.0. Student's t-test, two-way ANOVA and Log-rank were used to analyze significant differences in data. A *P* value < 0.05 was considered statistically significance.

Results

Characterization of Lipid Nanoparticles/Microparticles

Lipid particles with different particle sizes were successfully prepared. The structure of lipid/mRNA particles was shown in (Fig. 1a). The size and zeta potential of lipid particles were measured by DLS and DLS analysis showed that the particle size of small lipid/mRNA nanoparticles, formulated by solvent diffusion method, was approximately 90.15 ± 2.92 nm (PDI=0.21) and the zeta potential was approximately 8.03 ± 1.40 mV (Fig. 1b-d). The particle size of medium lipid/mRNA nanoparticles, formulated by microfluidics, was approximately 300 ± 40 nm (PDI=0.25), and the zeta potential was approximately 12.30 ± 1.03 mV (Fig. 1b, e and f). The particle size of large lipid/mRNA microparticles, formulated by film dispersion method, was approximately 1150 ± 100 nm (PDI=0.47), and the zeta potential was approximately 28.60 ± 2.20 mV (Fig. 1b, g and h). The results acquired from transmission electron microscope (TEM) showed similar as DLS analysis (Fig. 1i, j and k). In addition, the encapsulation efficiencies (EEs) of small, medium and larger size formulations were respectively 93.40%

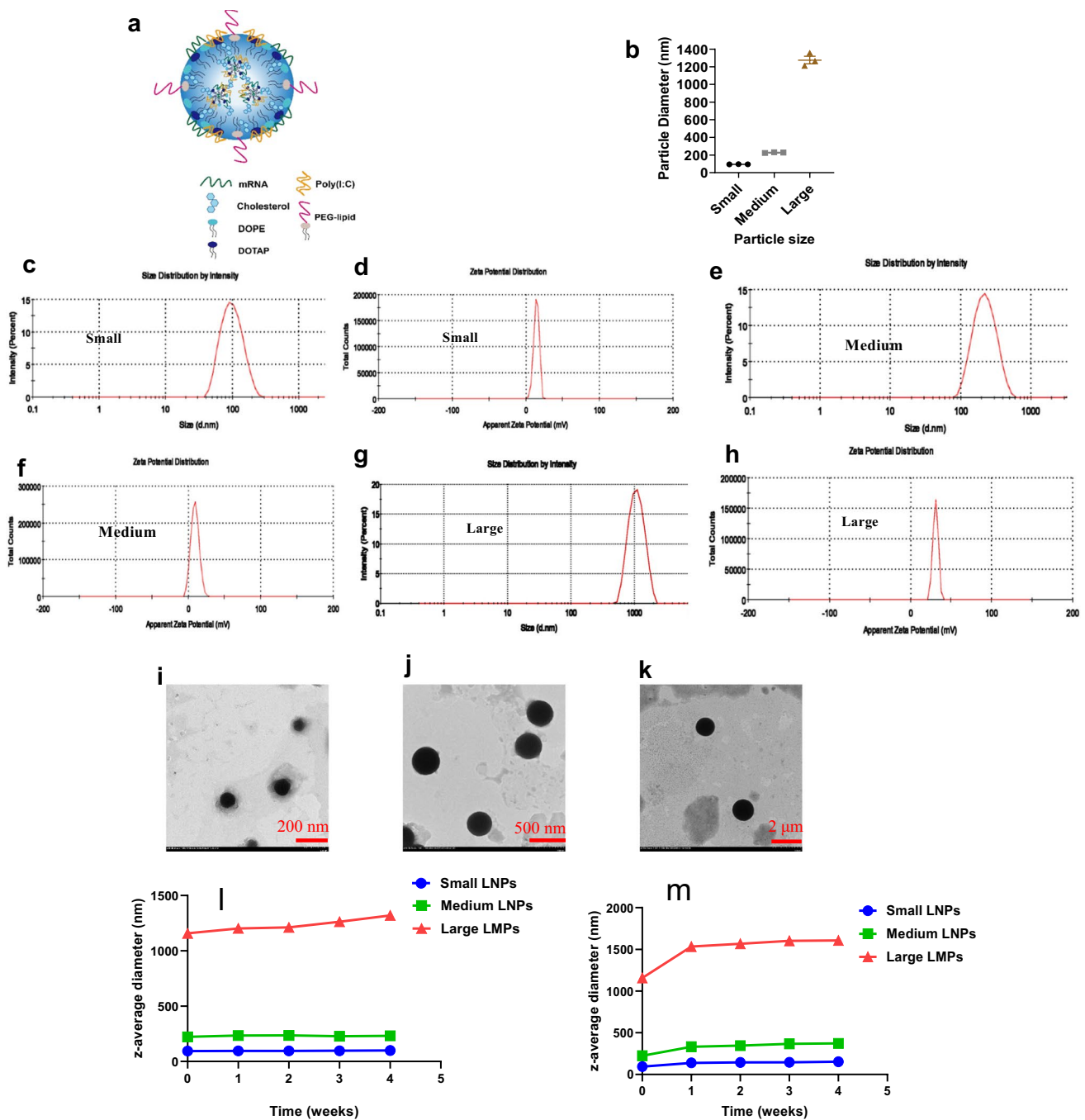


Fig. 1 Characterization of lipid/mRNA particles. (a). Schematic representation of a lipid particle consisting of lipids and mRNA. (b). The summary of particle size and PDI of lipid particles. (c) and (d). The size and zeta potential of small size lipid nanoparticles. (e) and (f). The size and zeta potential of medium size lipid nanoparticles. (g) and (h). The size and zeta potential of large size lipid microparticles. (i). The image of small size (around 90 nm) LNP captured by TEM. (j). The image of medium size (around 200 nm) LNP captured by TEM. (k). The image of large size (around 500 nm) LNP captured by TEM. (l). Investigation of stability of lipid particles on particle size under 4°C. m. Investigation of stability of lipid particles on particle size under -20°C.

(A-LNP), 88.70% (B-LNP) and 87.07% (C-LNP). The stability studies on particle size showed that LMPs have similar stability with LNPs when stored at 4 °C or -20 °C for 4 weeks (Fig. 1l and m). A slightly increase in z-average diameter was observed when freezing the lipid particles, indicating that freeze–thaw cycles should be avoided.

The Impact of Particle Size on Cellular Uptake of Lipid Particles *In Vitro*

In order to explore the cellular uptake properties of particles with different sizes, we utilized FITC-DSPE-PEG2000 instead of DMG-PEG2000 to prepare lipid particles.

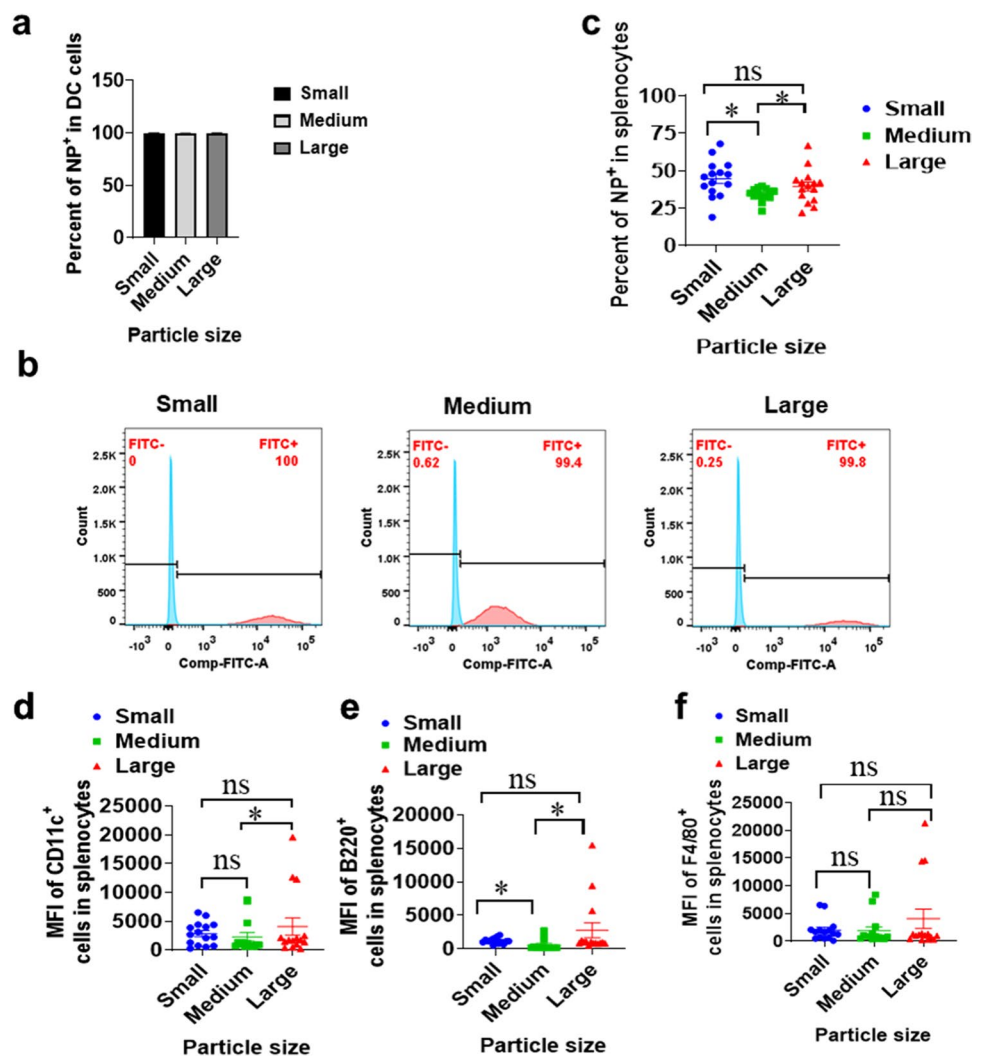
According to the analysis results, all 3 different lipid particles could be efficiently uptake by DC2.4 when co-incubation with DC2.4 cell lines (Fig. 2a and b). When we analyze the endocytosis of nanoparticles or microparticles by all antigen-presenting cells (APCs), including dendritic cells (DC), B cells and macrophages, we found that both small size lipid nanoparticles (90 nm LNP) and large size microparticles (1.2 μ m LMP) showed significant stronger uptake signals than medium size lipid nanoparticles (300 nm LNP) (Fig. 2c). In the study, we used PerCP/Cyanine5.5 anti-mouse CD11c antibody to label DC. APC anti-mouse B220 antibody and APC/Cyanine7 anti-mouse F4/80 antibody were applied to mark B cells and macrophages, respectively. DC is the most important APC in initiating cellular immunity and humoral immunity. In terms of DC uptake, we discovered that large size microparticles showed significant stronger uptake than medium size nanoparticles and the other comparing didn't show significant differences (Fig. 2d). In terms of B cell uptake, it was witnessed that

both small size lipid nanoparticles and large size microparticles showed significant stronger uptake signals than medium size lipid nanoparticles (Fig. 2e). However, all three size particles didn't show any significant difference in uptake by macrophages (Fig. 2f). These data indicated that small size lipid nanoparticles and large size microparticles can be uptake by total APCs stronger than medium size lipid nanoparticles.

The Impact of Particle Size on Transfection Efficiency *In Vitro*

To verify whether particle size can impact the efficacy of mRNA delivery, we tested the transfection efficacy of EGFP-mRNA after delivering by different size of lipid particles. The efficacy of mRNA delivery was examined by determining the quantity of transfected cells and the value of mean fluorescent intensity (MFI). As shown in Fig. 3a and b, all three sizes of lipid/mRNA particles

Fig. 2 Cellular uptake FITC-lipid complexes with different particle sizes. (a–b). The percentage of NP⁺ cells in DC2.4 live cells (n=6). (c). The percentage of NP⁺ cells in splenocytes (n=15). (d). The mean fluorescence intensity (MFI) of B220⁺ cells (B cells) in splenocytes. (e). The MFI of F4/80⁺ cells (macrophages) in splenocytes. (f). The MFI of CD11c⁺ cells (DC) in splenocytes. * means with significant difference and $P < 0.05$; ns means not significant.



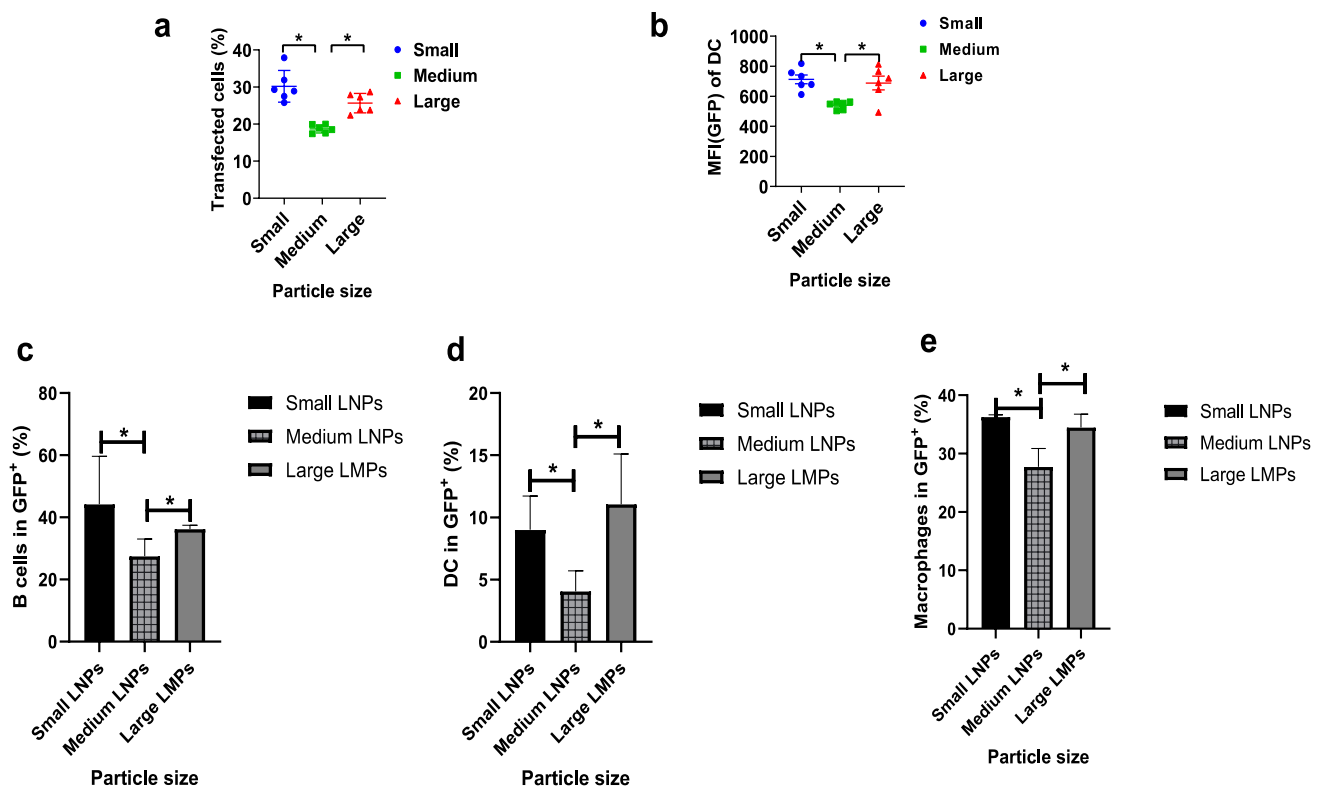


Fig. 3 Investigation of transfection efficiency of mRNA particles into DC2.4 ($n=6$) and investigation of transfection efficiency of mRNA particles into different antigen-presenting cells in splenocytes *in vivo* ($n=3$). (a–b). Expression of eGFP mRNA in DC2.4 cells and the corresponding transfection efficiency at 24 h after co-incubation with different lipid particles. (c). *In vivo* expression of eGFP mRNA in B cells of splenocytes at 24 h after splenocytes co-incubating with different lipid particles. (d). *In vivo* expression of eGFP mRNA in DC of splenocytes at 24 h after splenocytes co-incubating with different lipid particles. (e). *In vivo* expression of eGFP mRNA in macrophages at 24 h after splenocytes co-incubating with different lipid particles. *means significant difference and $P < 0.05$.

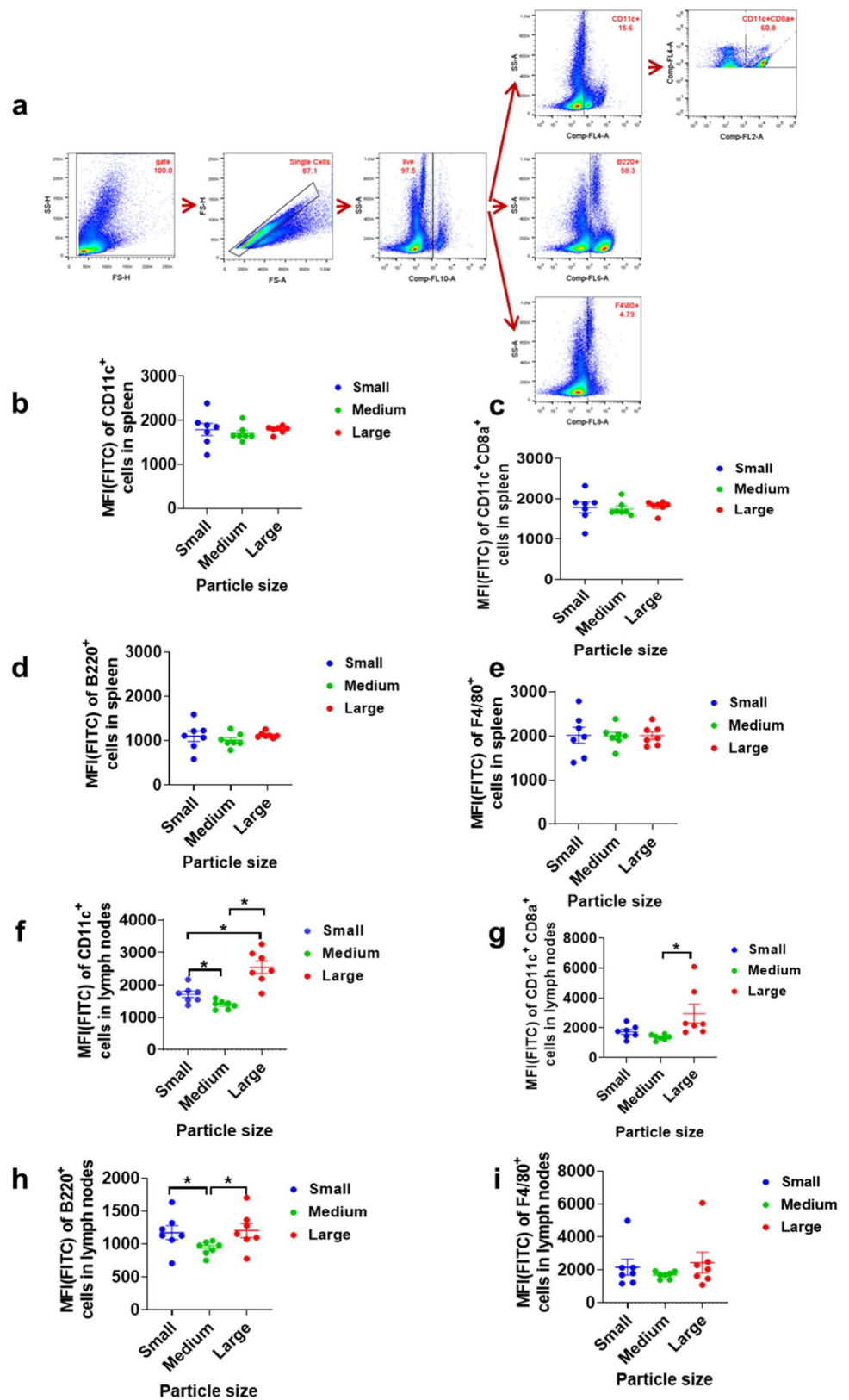
could deliver EGFP-mRNA to cells and cause the transfection of cells. However, compared to medium size lipid nanoparticles (300 nm LNP), small size nanoparticles (90 nm LNP) and large size microparticles (1.2 μ m LMP) demonstrated significantly higher transfection efficacy of EGFP-mRNA and induced transfections in more cells. These data illustrated that small size nanoparticles (90 nm LNP) and large size microparticles (1.2 μ m LMP) perform better *in vitro*.

Splenocytes were applied to analyze the transfection of different lipid particles, tanks to that splenocytes contain B cells, DC and macrophage. The results showed that the mRNA loaded lipid particles were efficiently uptake and expressed these 3 different antigen-presenting cells. As shown in Fig. 3c–e, there was no significant difference between small size (90 nm) and large size (1.2 μ m) lipid particles in the expression of mRNA in B cells, macrophage and DC cells. However, both small size (90 nm) and large size (1.2 μ m) lipid particles illustrated stronger expression of mRNA than that of medium size (300 nm) lipid particles in B cells, macrophage and DCs.

The Impact of Particle Size on Lipid Particle Uptake *In Vivo*

TO verify the results of endocytosis of lipid particles *in vitro*, we further conduct an *in vivo* experiment to study the impact of particle size on the uptake of particles APCs. The same as above, we used PerCP/Cyanine5.5 anti-mouse CD11c antibody to label DC and PE anti-mouse CD8a antibody to identify subgroup of DC related with induction of immune responses. APC anti-mouse B220 antibody and APC/Cyanine7 anti-mouse F4/80 antibody were applied to mark B cells and macrophages, respectively. The gating strategy in flow cytometric analysis is shown in Fig. 4a. Herein, besides CD11c⁺ DC population, CD11c⁺CD8⁺ DC population was also investigated to provide more comprehensively information, given that CD11c⁺CD8⁺ DCs is the population in DCs that play critical role in activating T cells and inducing the immune responses. The results revealed that no lipid particles produced a statistically different endocytosis efficiency with other size lipid particles in splenocytes *in vivo* (Fig. 4b–e). While in the investigation of lipid particle uptake

Fig. 4 The analysis of *in vivo* delivery efficiency of lipid particles with different sizes (n=7). **(a)** The gating strategy in flow cytometry studies. **(b-e)** The MFI (FITC) of DC, CD8a⁺ DC, B cells, and macrophage in splenocytes. **(f-i)** The MFI (FITC) of DC, CD8a⁺ DC, B cells, and macrophage in LNs. * means significance and *P* < 0.05.



by APC in lymph nodes, it was discovered that DC, CD8a⁺ DC and B cells, were more inclined to take up large lipid microparticles (1.2 μm LMPs) (Fig. 4f-i), though small size

lipid nanoparticle (90 nm LNP) also showed significantly higher uptake than medium size lipid nanoparticles (300 nm LNP). According to previous studies have reported that

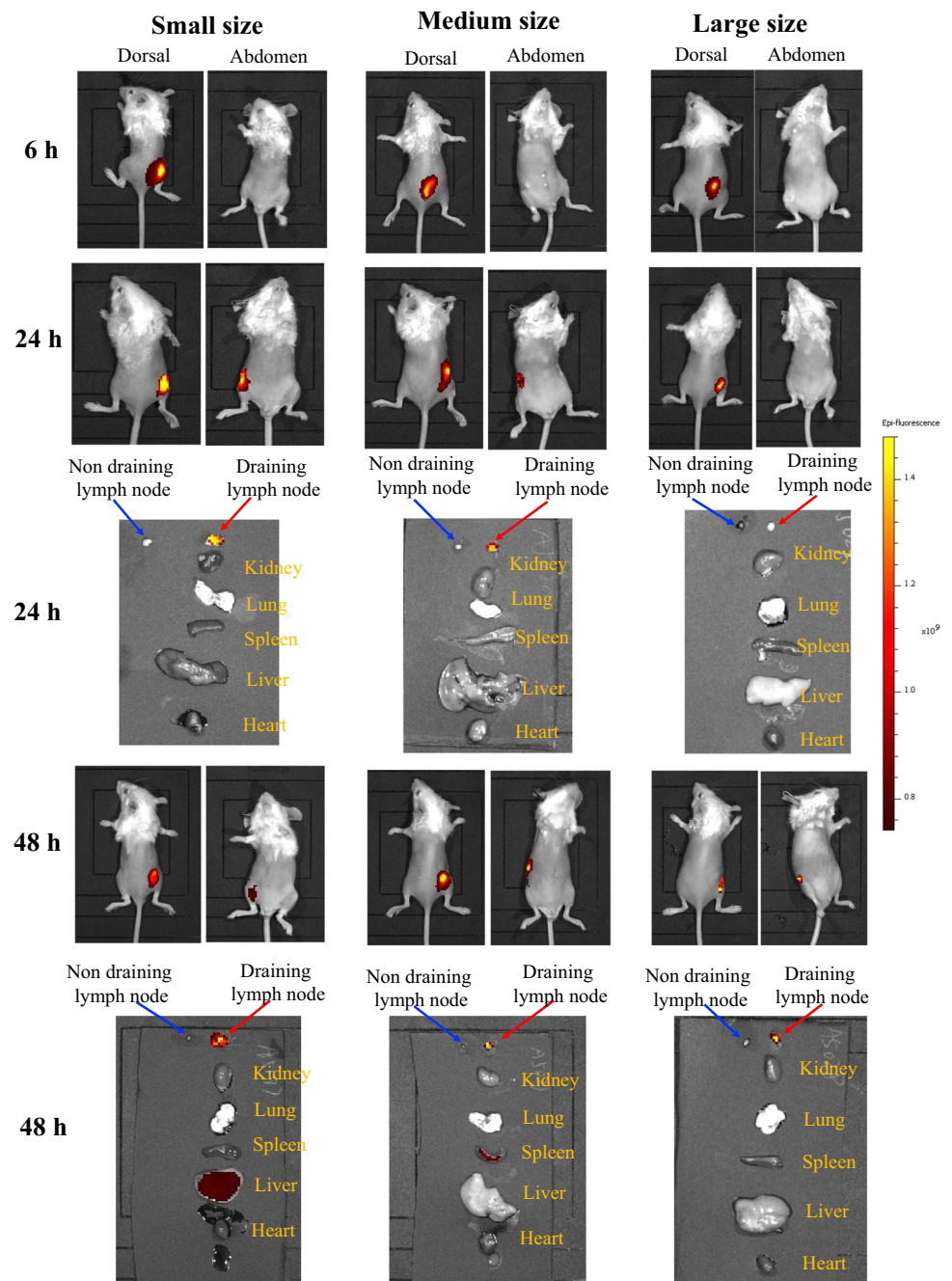
larger particles stay longer at the injection site, we suspect that micron-sized lipid microparticles have a greater chance of being taken up by antigen-presenting cells at the host site [1, 36, 37, 43–46].

Investigation of Biodistribution of Lipid Particles

In vivo imaging results (Fig. 5) showed that, micron-sized lipid particles may reside longer in injection site and draining lymph nodes than nano-sized lipid particles. 6 h after injection of lipid particles with three particle sizes,

fluorescence signals were observed at the injection site, and the fluorescence signals of the particles with small particle sizes tend to migrate to the draining lymph node. 24 h after injection, the fluorescence signal of draining lymph nodes could be observed obviously, which suggests that the complexes enter the draining lymph nodes from the injection site. 48 h after injection, the fluorescence signal in draining lymph nodes was enhanced in medium size LNP and large size LNP, but decreased in small size LNP. Meanwhile, fluorescent signals in various organs of mice revealed that draining lymph node has the highest

Fig. 5 Investigation of biodistribution of lipid particles after subcutaneously injected at the right back. Imaging *in vivo* is conducted at 6 h, 24 h and 48 h after the administration of lipid particles; the distribution of lipid particles in major organs is conducted at 24 h and 48 h after sacrificing the mice.



concentration of all 3 types of lipid particles. Besides, the micron-sized lipid particles remain in the lymph nodes, while the small size lipid particles have some migration to liver and medium size lipid particles have some distribution to spleen. These data suggest that lipid microparticles migrate to lymph nodes more slowly than small lipid nanoparticles.

The Impact of mRNA Vaccine Size on Preventing Cancer

To further investigate the impact of particle size on vaccine potency, we immunized mice with different size mRNA vaccines and then challenged mice with E.G7-OVA cancer cell, a cell line that can induce T lymphoma. Since, the mRNA in lipid particles can encode the antigen ovalbumin (OVA) and E.G7-OVA cancer cell express the antigen OVA, immunize mice with mRNA vaccines would induce OVA-specific immune responses and thus retard the tumor growth.

In the study, mice were vaccinated on day -28 and day -21 with OVA mRNA vaccines, and then on day 0 the mice were subcutaneously inoculated with OVA expressing E.G7 lymphoma cells (Fig. 6a). The tumor growth and survival rate of mice were monitored to evaluate the efficacy of different size mRNA vaccines. As tumor growth curves and survival curve shown in Fig. 6b and c, mice vaccinated with different sized lipid particles showed a significant delay of tumor growth and a prolongation of survival, compared with the mice in PBS control group and blank nanoparticle group. However, there was no significant difference, in terms of tumor growth and mouse survival, between mRNA vaccines with different particle size. Besides, it should be noted that immune adjuvants, either poly(I:C) or hesperetin, could improve the efficacy of mRNA vaccines (Fig. 6d and e), though the cationic lipids in mRNA formulation themselves have partial adjuvant function. Poly(I:C) and hesperetin are easy to be encapsulated into mRNA formulation due to they are also negatively charged, which is the same as mRNA.

The data demonstrated that there was no significant difference between mRNA vaccines encapsulated with poly(I:C) group and mRNA vaccines encapsulated with hesperetin. (Fig. 6d and e). Hesperetin is an active substance from traditional Chinese medicine and potentially has the ability to alter immune responses. The study presented here indicated that hesperetin potentially could be applied as immune adjuvants.

Furthermore, the cellular immunity and antigen-specific T cells induced by mRNA vaccines were analyzed by detecting the IFN- γ secreting CD8⁺ or CD4⁺ T cells upon stimulating by incubating with OVA peptides antigens. IFN- γ secreting is the sign of T cell activation, therefore we can quantify the amounts of activated antigen-specific T cells by mixing antigens with immune cells. The results showed that the percentage of IFN- γ ⁺CD8⁺ T cells in mice, immunized

by all 3 sizes of mRNA vaccines, are higher than that in the PBS control group (Fig. 6f). Meanwhile, the percentage of IFN- γ ⁺ CD4⁺ T cells in mice, immunized by large microparticles, was significantly higher than that in the PBS control group (Fig. 6g). These results indicated that all 3 size lipid particles can effectively activate antigen-specific cellular immunity.

Investigation of Antigen-Specific Humoral Immunity Induced by mRNA Vaccines

To evaluate the impact of particle size on inducing antigen-specific humoral immunity, the OVA-specific IgG concentrations in serum of mice were measured after immunizing mice with mRNA vaccines. In this study, all 3 kinds of mRNA vaccines induced robust humoral immune responses and statistically difference was observed between different vaccine groups (Fig. 7a). Meanwhile, comparing with PBS control group and medium blank nanoparticle control group, it was found that medium lipid nanoparticles without adjuvants can also induced stronger humoral immunity, and the addition of adjuvant hesperetin didn't increase the humoral immune response (Fig. 7b). These data indicated that in terms of inducing humoral immunity, 90 nm lipid nanoparticle (LNP), 300 nm lipid nanoparticle (LNP) and 1.2 μ m lipid microparticle (LMP) have no significance. In addition, the lipids included in the particles also worked as adjuvants in facilitating the activation of humoral immunity.

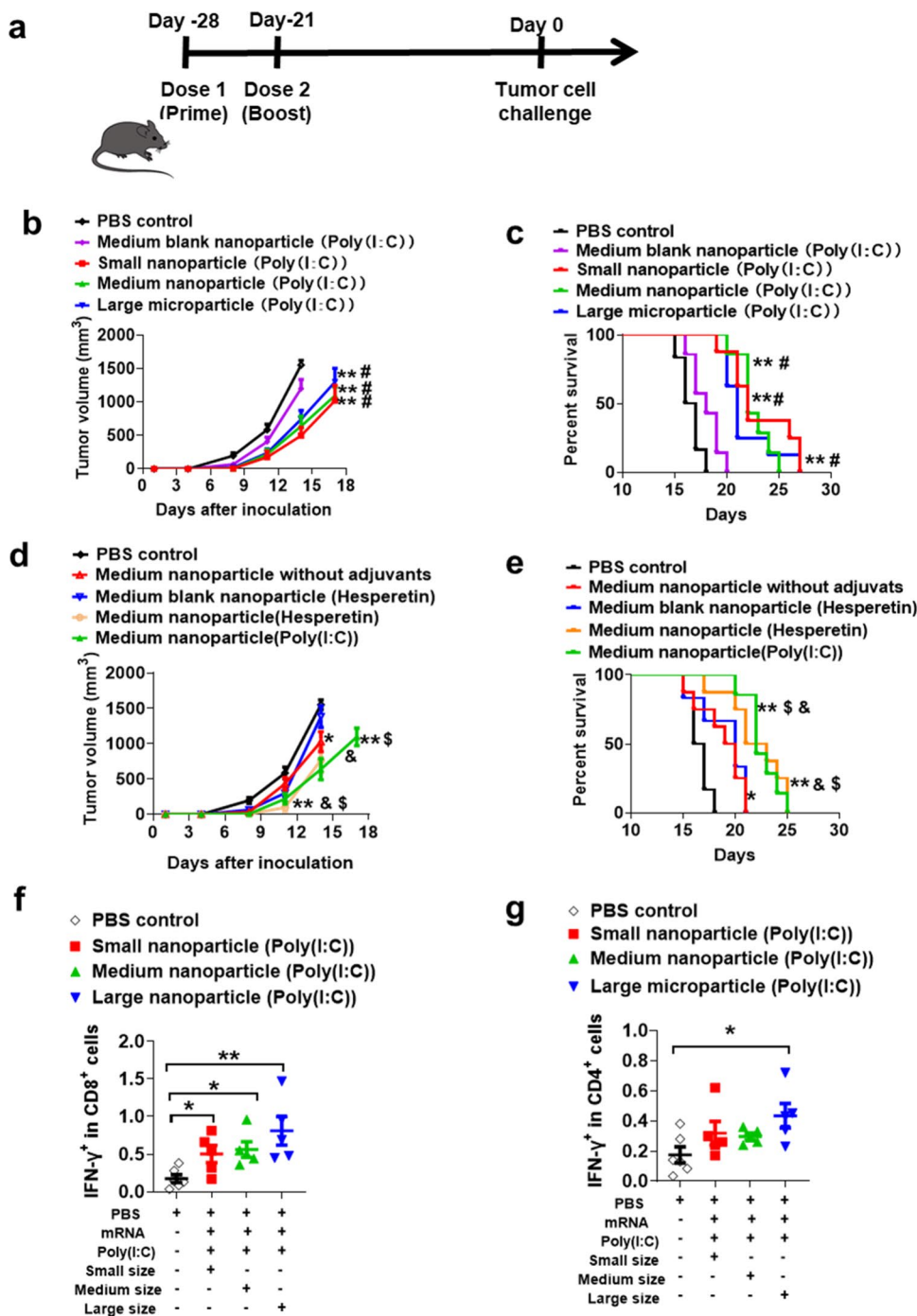
Analysis of Toxicity to Major Organs During Immunization

To assess the potential side effects of lipid nanoparticles or lipid microparticles, the major organs were analyzed by H&E staining after vaccine immunization. As shown in Fig. 7c, no obvious pathological changes or toxicities were observed in the collected tissue samples, including heart, liver, spleen, lung and kidney.

Discussions and Conclusions

Thank to mRNA vaccine platform presents various advantages, such as good safety, rapid manufacture, and co-induction of cellular and humoral responses etc., the studies on mRNA therapy are becoming hot spot and entering a very exciting stage [42, 47]. Once injected through subcutaneously or intramuscularly, mRNA vaccines are uptake by APCs and then transported to the draining lymph nodes (dLNs) by migratory APCs [48]. The crucial APCs for the induction of cellular immunity and humoral immunity are DCs, which are highly specialized to take up and process

Fig. 6 Analysis of prevention efficacy of mRNA lipid particles with different sizes. **(a)**, Time line of the mice immunization and tumor inoculation. **(b-c)**, Tumor growth curve and survival rate of mice immunized with different size mRNA vaccines (n=8). **(d-e)**, Tumor growth curve and survival rate of mice immunized with mRNA vaccines encapsulated with different adjuvants (n=8). **(f-g)**, Measurement of IFN- γ secreting CD8⁺ and CD4⁺ T lymphocytes in splenocytes after stimulating by OVA peptides. *and ** mean compared with PBS control group; # means compared with medium blank nanoparticle loaded with only poly(I:C); \$ means compared with medium blank nanoparticle loaded with hesperetin; & means compared with medium nanoparticle without adjuvants. *, #, & and \$, P < 0.05; ** P < 0.01.



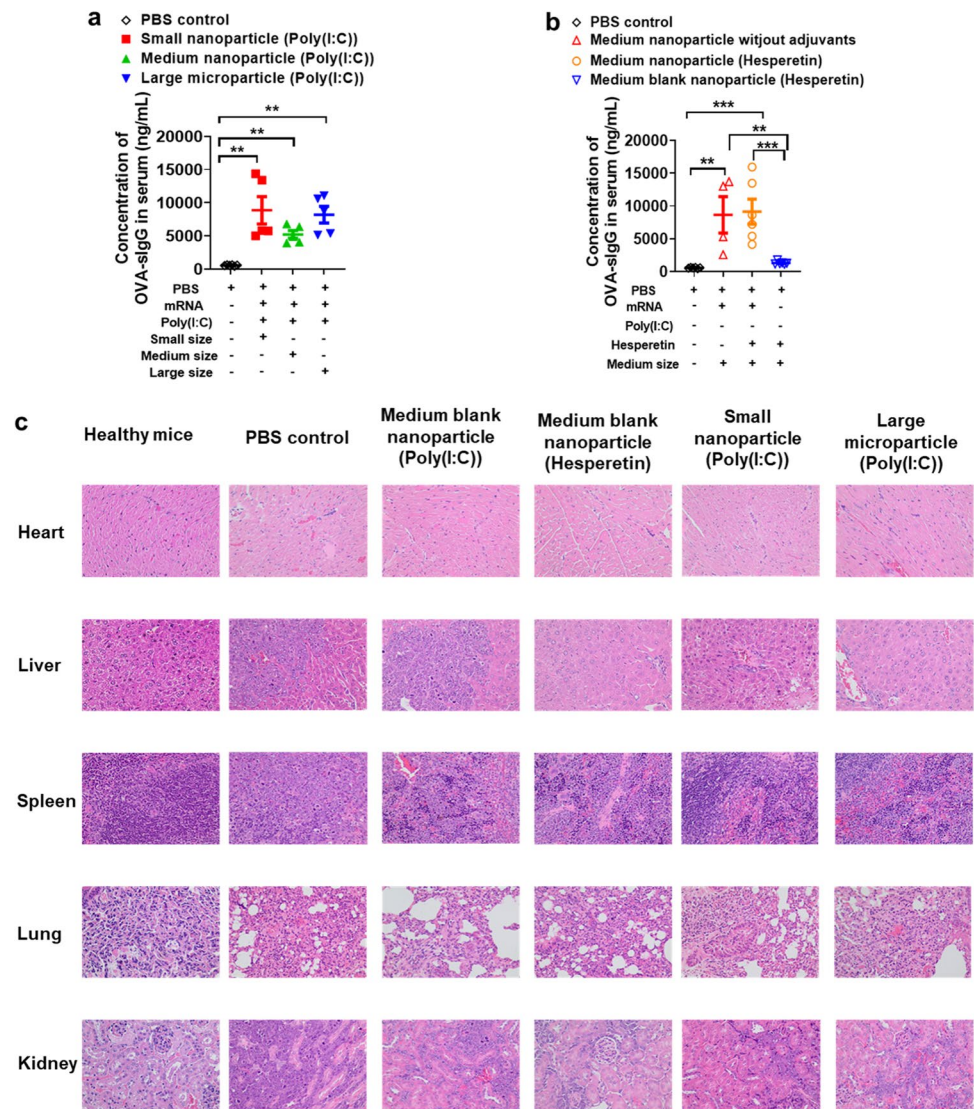
antigens [1, 45, 49–51]. The efficient uptake of antigen or its delivery platform by APCs depends on properties of particles, such as the size of particles [1, 51].

In reported studies and the FDA-approved mRNA vaccines, scientists applied lipid nanoparticles with the size around 70 nm-100 nm. No researches have compared the impact of particle size on the efficacy of lipid particles in a broader range. Therefore, we compared the efficacy of lipid microparticles (LMPs) with LNPs in delivering mRNA.

In the studies, there typical particle sizes were applied, 90 nm, 300 nm and 1.2 μ m. Thus, both lipid nanoparticles (LNP) and lipid microparticles (LMPs) were included. 90 nm LNPs and 1.2 μ m LMPs showed stronger cellular uptake and transfection than 300 nm LNPs *in vitro*.

APCs can take up mRNA lipid particles at both the injection site and draining lymph nodes. Particle size determines the mechanism of trafficking to the lymph nodes. According to previous studies, nanoparticles traffic to the draining

Fig. 7 Analysis antigen-specific humoral immunity induced by lipid nanoparticles or microparticles and evaluation of toxicities of mRNA vaccines by H&E staining. (a–b), Analysis antigen-specific humoral immunity induced by lipid nanoparticles or microparticles by measuring the concentrations of OVA-specific IgG in serum of mice. (c), evaluation of toxicities of mRNA vaccines by H&E staining of major organs (Each figure has at least 3 repeats and the figures are representative one from these 3 repeats). **and *** mean compared with PBS control group; ** means $P < 0.01$; *** means $P < 0.005$.



lymph nodes in a size-dependent manner, the smaller size (smaller than 200 nm) particles can infiltrate into lymph node more easily than larger particles. Whereas, lipid microparticles were uptake similarly by the DCs in lymph node with small size lipid nanoparticles (90 nm). We speculate that this is duo to large microparticles (500 nm—2000 nm) mostly uptake by DCs from the injection site and these DCs carried the lipid microparticles into the lymph node [37, 44, 46]. Literature suggests that lipid nanoparticles smaller than 200 nm freely drain to the lymph nodes [1, 43, 45, 46, 51, 52]. Previous studies showed that smaller lipid particles leave the injection site more readily than larger particles, however, smaller lipid complexes in the 30 nm size range drain rapidly from the site of s.c injection resulting in limited potency [53]. Lipid nanoparticles, with size 30 nm -200 nm, most are uptake by APCs in lymph node and with a part of nanoparticles uptake by APCs at injection site [1, 43]. Theoretically, large lipid microparticles can

recruit circulating APCs, such as DCs, and uptake by such APCs, followed by being carried into the lymphatic system by APCs which can squeeze through openings between overlapping endothelial cells [1, 52, 54–58]. So far, limited knowledge exists for whether micron-sized lipid microparticles could be used to deliver mRNA and how it impacts vaccine potency. Given the above situations, our studies, comparing lipid microparticles with lipid nanoparticles in delivering mRNA, provided important information in mRNA delivering area for deeper investigations.

According to our *in vivo* immunization study, all 3 sized mRNA vaccines could induce effective immune responses and showed a significant delay of tumor growth in preventing cancer on mouse model. Besides, significant difference in cellular immunogenicity and humoral immunogenicity was observed between these 3 different lipid nanoparticles (LNPs) and lipid microparticles (LMPs). According to previous studies and our studies on nanoparticles and microparticles, we

speculate that these results were caused by the combination of different residence time of particles stay in injecting site and ability of particles infiltrating into lymph node [1, 37, 43–46].

In summary, we prepared 3 different size lipid/mRNA particles without changing their lipid composition. It was witnessed that lipid/mRNA particles encapsulating with immune adjuvants (either poly(I:C) or hesperetin) showed a more significant stronger immune responses than lipid particles without adjuvants. Notably, compared to the most commonly used 50–100 nm lipid nanoparticles (LNP), 1–2 µm sized lipid/mRNA microparticles (LMP) showed similar robust immune response and excellent intracellular delivery. 50–100 nm lipid nanoparticles (LNP) have been approved to be applied in clinic to deliver mRNA vaccines. Therefore, this work proved that lipid microparticles can achieve similar mRNA delivery efficacy with small size lipid nanoparticles, and thus provided us an alternative micron-sized platform for mRNA delivery, besides lipid nanoparticles with size smaller than 150 nm.

Fundings

This research was funded by Priority Academic Program Development (PAPD) of Jiangsu Higher Education Institutions, the Health Talent Training Project of Suzhou (GSWS2019069, GSWS2020094) and Suzhou Science and Technology Development Project for People's Livelihood (SS202011).

Author Contributions Conceptualization, M.L.; methodology, M.L, A.J, M.X, Y.P, and L.D.; software, A.J, M.X and L.M; validation, M.X., L.M. and L.M.; formal analysis, M.X, A.J.; investigation, A.J, M.X. and Y.P; resources, M.L and J.C.; data curation, A.J., M.X, and M.X; writing—original draft preparation, A.J.; writing—review and editing, M.L, M.X, and L.Q.; supervision, M.L. and J.C; project administration, M.L.; funding acquisition, M.L and J.C. All authors have read and agreed to the published version of the manuscript.

Data Availability The data supporting the findings of this study are included in the paper. All other relevant data are available from the corresponding author upon reasonable request.

Declarations

Animal Study Statement All animal work was approved and monitored by the Animal Ethics Committee of Soochow University.

Conflicts of Interest The authors declare no conflict of interests.

References

- Bachmann MF, Jennings GT. Vaccine delivery: a matter of size, geometry, kinetics and molecular patterns. *Nat Rev Immunol*. 2010;10:787–96.
- Wibawa T. COVID-19 vaccine research and development: ethical issues. *Trop Med Int Health*. 2021;26:14–9.
- Zhang CL, Maruggi G, Shan H, Li JW. Advances in mRNA Vaccines for Infectious Diseases. *Front Immunol*. 2019;10.
- Pardi N, Hogan MJ, Porter FW, Weissman D. mRNA vaccines - a new era in vaccinology. *Nat Rev Drug Discov*. 2018;17:261–79.
- Grunwitz C, Kranz LM. mRNA Cancer Vaccines—Messages that Prevail. *Curr Top Microbiol*. 2017;405:145–64.
- Miao L, Zhang Y, Huang L. mRNA vaccine for cancer immunotherapy. *Mol Cancer* 2021;20.
- Chandler M, Johnson MB, Panigaj M, Afonin KA. Innate immune responses triggered by nucleic acids inspire the design of immunomodulatory nucleic acid nanoparticles (NANPs). *Curr Opin Biotech*. 2020;63:8–15.
- Kim J, Eygeris Y, Gupta M, Sahay G. Self-assembled mRNA vaccines. *Adv Drug Deliver Rev*. 2021;170:83–112.
- Wadhwa A, Aljabbari A, Lokras A, Foged C, Thakur A. Opportunities and Challenges in the Delivery of mRNA-Based Vaccines. *Pharmaceutics* 2020;12.
- Soleimanpour S, Yaghoubi A. COVID-19 vaccine: where are we now and where should we go? *Expert Rev Vaccines*. 2021;20:23–44.
- Buschmann MD, *et al*. Nanomaterial delivery systems for mRNA vaccines. *Vaccines-Basel* 9(2021).
- Kariko K, *et al*. Incorporation of pseudouridine into mRNA yields superior nonimmunogenic vector with increased translational capacity and biological stability. *Mol Ther*. 2008;16:1833–40.
- Guan S, Rosenecker J. Nanotechnologies in delivery of mRNA therapeutics using nonviral vector-based delivery systems. *Gene Ther*. 2017;24:133–43.
- Kauffman KJ, Webber MJ, Anderson DG. Materials for non-viral intracellular delivery of messenger RNA therapeutics. *J Control Release*. 2016;240:227–34.
- John S, *et al*. Multi-antigenic human cytomegalovirus mRNA vaccines that elicit potent humoral and cell-mediated immunity. *Vaccine*. 2018;36:1689–99.
- Hassett KJ, *et al*. Optimization of lipid nanoparticles for intramuscular administration of mRNA vaccines. *Mol Ther-Nucl Acids*. 2019;15:1–11.
- Reichmuth AM, Oberli MA, Jaklenec A, Langer R, Blankschtein D. mRNA vaccine delivery using lipid nanoparticles. *Ther Deliv*. 2016;7:319–34.
- Sabnis S, *et al*. A novel amino lipid series for mRNA delivery: improved endosomal escape and sustained pharmacology and safety in non-human primates. *Mol Ther*. 2018;26:1509–19.
- Richner JM, *et al*. Modified mRNA vaccines protect against Zika Virus Infection. *Cell* 2017;168:1114–+.
- Guevara ML, Persano F, Persano S. Advances in lipid nanoparticles for mRNA-based cancer immunotherapy. *Front Chem*. 2020;8.
- Samaridou E, Heyes J, Lutwyche P. Lipid nanoparticles for nucleic acid delivery: Current perspectives. *Adv Drug Deliver Rev*. 2020;154:37–63.
- Pardi N, *et al*. Expression kinetics of nucleoside-modified mRNA delivered in lipid nanoparticles to mice by various routes. *J Control Release*. 2015;217:345–51.
- Siewert CD, *et al*. hybrid biopolymer and lipid nanoparticles with improved transfection efficacy for mRNA. *Cells-Basel* 2020;9.
- Oberli MA, *et al*. Lipid nanoparticle assisted mRNA delivery for potent cancer immunotherapy. *Nano Lett*. 2017;17:1326–35.
- Hassett KJ, *et al*. Impact of lipid nanoparticle size on mRNA vaccine immunogenicity. *J Control Release*. 2021;335:237–46.

26. Malyala P, O'Hagan DT, Singh M. Enhancing the therapeutic efficacy of CpG oligonucleotides using biodegradable microparticles. *Adv Drug Deliv Rev.* 2009;61:218–25.
27. Fischer T, *et al.* siRNA delivery to macrophages using aspherical, nanostructured microparticles as delivery system for pulmonary administration. *Eur J Pharm Biopharm.* 2021;158:284–93.
28. Hinkelmann S, *et al.* Mineralizing gelatin microparticles as cell carrier and drug delivery system for siRNA for bone tissue engineering. *Pharmaceutics* 2022;14.
29. Shen J, *et al.* Porous silicon microparticles for delivery of siRNA therapeutics. *J Vis Exp.* 2015;52075.
30. Fischer T, Winter I, Drumm R, Schneider M. Cylindrical microparticles composed of mesoporous silica nanoparticles for the targeted delivery of a small molecule and a macromolecular drug to the lungs: exemplified with curcumin and siRNA. *Pharmaceutics* 2021;13.
31. Wang Q, Tan MT, Keegan BP, Barry MA, Heffernan MJ. Time course study of the antigen-specific immune response to a PLGA microparticle vaccine formulation. *Biomaterials.* 2014;35:8385–93.
32. Garlapati S, *et al.* PCPP (poly[di(carboxylatophenoxy)-phosphazene]) microparticles co-encapsulating ovalbumin and CpG oligo-deoxynucleotides are potent enhancers of antigen specific Th1 immune responses in mice. *Vaccine.* 2010;28:8306–14.
33. Zhang XQ, *et al.* Potent antigen-specific immune responses stimulated by codelivery of CpG ODN and antigens in degradable microparticles. *J Immunother.* 2007;30:469–78.
34. Guo J, *et al.* Chitosan microsphere used as an effective system to deliver a linked antigenic peptides vaccine protect mice against acute and chronic toxoplasmosis. *Front Cell Infect Microbiol.* 2018;8:163.
35. Carcaboso AM, *et al.* Potent, long lasting systemic antibody levels and mixed Th1/Th2 immune response after nasal immunization with malaria antigen loaded PLGA microparticles. *Vaccine.* 2004;22:1423–32.
36. Norling LV, Dalli J. Microparticles are novel effectors of immunity. *Curr Opin Pharmacol.* 2013;13:570–5.
37. Benne N, van Duijn J, Kuiper J, Jiskoot W, Slutter B. Orchestrating immune responses: How size, shape and rigidity affect the immunogenicity of particulate vaccines. *J Control Release.* 2016;234:124–34.
38. Henriksen-Lacey M, Devitt A, Perrie Y. The vesicle size of DDA:TDB liposomal adjuvants plays a role in the cell-mediated immune response but has no significant effect on antibody production. *J Control Release.* 2011;154:131–7.
39. Wendorf J, *et al.* A comparison of anionic nanoparticles and microparticles as vaccine delivery systems. *Hum Vaccin.* 2008;4:44–9.
40. Mann JF, *et al.* Lipid vesicle size of an oral influenza vaccine delivery vehicle influences the Th1/Th2 bias in the immune response and protection against infection. *Vaccine.* 2009;27:3643–9.
41. Brewer JM, Pollock KG, Tetley L, Russell DG. Vesicle size influences the trafficking, processing, and presentation of antigens in lipid vesicles. *J Immunol.* 2004;173:6143–50.
42. Zhang R, *et al.* DP7-C-modified liposomes enhance immune responses and the antitumor effect of a neoantigen-based mRNA vaccine. *J Control Release.* 2020;328:210–21.
43. Pflücke H, Sixt M. Preformed portals facilitate dendritic cell entry into afferent lymphatic vessels. *Eur J Cell Biol.* 2009;88:76–7.
44. Di J, *et al.* Biodistribution and non-linear gene expression of mRNA LNPs affected by delivery route and particle size. *Pharm Res.* 2022;39:105–14.
45. Pozzi LAM, Maciaszek JW, Rock KL. Both dendritic cells and macrophages can stimulate naive CD8 T cells in vivo to proliferate, develop effector function, and differentiate into memory cells. *J Immunol.* 2005;175:2071–81.
46. Manolova V, *et al.* Nanoparticles target distinct dendritic cell populations according to their size. *Eur J Immunol.* 2008;38:1404–13.
47. Linares-Fernandez S, Lacroix C, Exposito JY, Verrier B. Tailoring mRNA vaccine to balance innate/adaptive immune response. *Trends Mol Med.* 2020;26:311–23.
48. Kowalczyk A, *et al.* Self-adjuvanted mRNA vaccines induce local innate immune responses that lead to a potent and boostable adaptive immunity. *Vaccine.* 2016;34:3882–93.
49. De Beuckelaer A, *et al.* Type I interferons interfere with the capacity of mRNA lipoplex vaccines to elicit cytolytic t cell responses. *Mol Ther.* 2016;24:2012–20.
50. Liang F, *et al.* Efficient targeting and activation of antigen presenting cells in vivo after modified mRNA vaccine administration in rhesus macaques. *Mol Ther.* 2017;25:2635–47.
51. Ahsan FL, Rivas IP, Khan MA, Suarez AIT. Targeting to macrophages: role of physicochemical properties of particulate carriers-liposomes and microspheres-on the phagocytosis by macrophages. *J Control Release.* 2002;79:29–40.
52. Swartz MA. The physiology of the lymphatic system. *Adv Drug Deliver Rev.* 2001;50:3–20.
53. Chen S, *et al.* Development of lipid nanoparticle formulations of siRNA for hepatocyte gene silencing following subcutaneous administration. *J Control Release.* 2014;196:106–12.
54. Yan SY, Gu WY, Xu ZP. Re-considering how particle size and other properties of antigen-adjuvant complexes impact on the immune responses. *J Colloid Interf Sci.* 2013;395:1–10.
55. Thomas C, Gupta V, Ahsan F. Particle size influences the immune response produced by hepatitis b vaccine formulated in inhalable particles. *Pharm Res-Dordr.* 2010;27:905–19.
56. Oyewumi MO, Kumar A, Cui ZR. Nano-microparticles as immune adjuvants: correlating particle sizes and the resultant immune responses. *Expert Rev Vaccines.* 2010;9:1095–107.
57. Katare YK, Muthukumaran T, Panda AK. Influence of particle size, antigen load, dose and additional adjuvant on the immune response from antigen loaded PLA microparticles. *Int J Pharmaceut.* 2005;301:149–60.
58. Jia CC, *et al.* A novel human papillomavirus 16 L1 pentamer-loaded hybrid particles vaccine system: influence of size on immune responses. *ACS Appl Mater Inter.* 2018;10:35745–59.

Publisher's Note Springer Nature remains neutral with regard to jurisdictional claims in published maps and institutional affiliations.

Springer Nature or its licensor (e.g. a society or other partner) holds exclusive rights to this article under a publishing agreement with the author(s) or other rightsholder(s); author self-archiving of the accepted manuscript version of this article is solely governed by the terms of such publishing agreement and applicable law.